(REVIEW ARTICLE)

# Wetability and dielectric property of DL-PLA/CLOISITE 20A/PANI nanocomposite

M. K. Panigrahi [1, *], R.I. Ganguly [2] and R.R. Dash [3]

[1] Department Materials Science, Maharaja Sriram Chandra Bhanja Deo University, Keonjhar Campus, Odisha, India.
[2] Department of Metallurgical Engineering, National Institute of Technology, Raurkela, Odisha, India.
[3] CSIR-National Metallurgical Laboratory (CSIR-NML), Jamshedpur, Jharkhand, India.

## Abstract

DL-PLA/CLOISITE 20A nanocomposite is fabricated by solution casting method. , DL-PLA/CLOISITE 20A/PANI Nanocomposite is also synthesized by chemical-oxidation method. Characterization of that nanocomposite is made using XRD, FTIR, UV Visible. TGA studies a wettability studies and dielectric analysis of prepared materials. Results reveal enhancement of thermal stability and crystallinity of the nanocomposite. Further, nanocomposite shows that it is hydrophilic in nature. Frequency dependent ac-conductivity and dielectric loss are estimated for the nanocomposite. Dielectric loss is observed to possess low value (0.2). Fabricated DL-PLA/Cloisite 20A may serve as insulating layers to suppress dielectric loss effectively.

## 1. Introduction

Microelectronic packaging materials are required to fulfill different other requirements such as low dielectric loss, moderate relative permittivity, moisture absorption resistance, low co-efficient of thermal expansion (CTE), high dimensional stability and mechanical stiffness [1]. For this purpose, ceramic-polymer composites are considered to be suitable for meeting functional packages which combine electrical properties of ceramic, mechanical flexibility, chemical stability, and processing possibilities of polymers. This material shows prospects for use in piezoelectric & pyrroelectric applications, flexible sensors, transducers, thick film dielectrics, embedded capacitors, tunable antennas and other multilayer radio frequency (RF) devices [2–4]. Presently, research is focused on polymer-ceramic composites [5–8]. Required polymer may be one of the followings i.e. PVDF [9], (PVDF–TrFE) [10], silicon-rubber [11], polyimide [12], polyvinyl chloride (PVC) [13], cyanoethylated cellulose polymer (CR-S) [14], polystyrene [15], and polyurethane [16]. However, only for a few composites, thermoplastic polymers are used [17, 18]. Due to their excellent chemical stability and good mechanical processing possibilities, they are net-shaped at elevated temperatures. Using injection molding, lamination or extrusion process, sheets or a 3D structure can be formed from these materials. Usually, thermoplastic polymers are suitable candidates for making ceramic-polymer composites.

Electronic waste has been causing environmental pollution during last few decades. If such materials are made from biodegradable polymer, then problems for environmental pollution due to electronic waste will be addressed. Such biodegradable polymers will be derived from renewable resources such as corn starch and sugar [19]. For this, polylactide (PLA) is considered to have suitability for applications in inverters, transistors and memories [20-23]. PLA is a type of thermoplastic polyester synthesized by ring-opening polymerization of lactide. All reasons stated above have derived numerous attentions from both industries and academia. Materials, thus developed, will have biodegradability,

---

biocompatibility, and improved mechanical performance with low cost of production [23-25]. However, poor dielectric performance of PLA restricts its extensive applications [26].

PLA has additional advantage of having good thermal stability and mechanical stability. One of the limiting factors of its use is lower permeability for gases, vapors and organic molecules having lower molecular weight [27]. Passage of oxygen and water vapor through polymer films drastically lowers service performance of a packaging material. This will cause difficulty to maintain food quality throughout its shelf life [28, 29]. Therefore, mass transfer through these polymers is an important consideration for development. Research is being carried out in this direction. Incorporation of two-dimensional (2D) platelets or disk-shaped nanoparticles in the polymer matrix has proven to be an advantageous strategy. The strategy has paid dividend by decreasing gas/liquid permeation in polymers. 2D platelets or disk-shaped nanoparticles act as physical barriers to diffusion path of the permeant molecule and therefore, creating a tortuosity effect. Food shelf-life increases by enhancing material performance [30-33]. Nanoclays such as mica, saponite, montmorillonite and kaolinite are used as 2D nanoparticles which improves barrier properties in many polymers [34]. There are many publications available on PLA/Clay nanocomposites. This composite is mainly focused on improving thermal [35-37], mechanical [38-40] and optical properties [41, 42]. Such material is also biodegradable [43, 44]. Comparatively fewer studies have been devoted to mass transfer in PLA, and PLA/clay nanocomposites.

Use of nanofillers like clays and silicates is advocated since they are available in abundance with low cost. Due to a few other reasons such as high aspect ratio, rich intercalation chemistry, high strength & stiffness, thermal stability, etc., they provide synergetic effects which help significantly to improve properties for many polymers [45-48]. However, properties largely depend on dispersion of clay layers in the polymer matrix. Intercalation, exfoliation, mixed intercalation & exfoliation, aggregation, etc. greatly affect gas barrier properties. Therefore, a high level of exfoliation with desired orientation of platelets remains a challenging task [49-52]. Healthy dispersion is feasible by increasing affinity between clay layers and polymer through organic modification of interlayer galleries. Affinity is improved by addition of organic ammonium, sulfonium or phosphonium cations. A Detailed list of common organic modifiers is suggested by Nordqvist and Hedenqvist [34]. Common dispersion of organo-modified layered silicates in a PLA matrix is achieved by adopting solution intercalation, melt processing and in situ polymerization methods [53].

Improvement in dielectric properties of PLA is achieved by preparing percolative composites with conductive fillers [54]. High dielectric constant near the percolation threshold is due to conductive fillers which act as micro-capacitors in the insulating polymer matrix [55-57]. However, composites suffer from high dielectric loss and low breakdown strength due to tunneling effect and direct Ohmic contact between pristine conductive fillers [58].

Easiest technique for preparation of nanocomposites in a laboratory scale is Solution intercalation method. In this method, clay platelets are exfoliated in a solvent in soluble polymer. Clay suspension in polymer solution is made where polymer chains adsorb on the surface of the platelets. Thus, clay-polymer complex is formed. Remaining evaporated leaves behind clay-polymer complex. However, the method is environmentally unfriendly due to escaping of organic solvents in the atmosphere [52]. Maharana et al. [59] have prepared PLA/clay nanocomposites using a solution intercalation method. Thus, the nanocomposite has shown better mechanical and barrier properties.

Effect of structure of different organic modifiers of clay nanoparticles such as Cloisite-15A, -25A and -30B modified with dimethyl dihydrogenated tallow quaternary ammonium, dimethyl hydrogenated tallow-2-ethylhexyl ammonium and methyl tallow-bis-2-hydroxyethyl quaternary ammonium have been studied by Pochan and Krikorian [60]. They have determined extent of exfoliation of nanoclay in a PLA matrix by solvent intercalation method.

Conducting polymers are new generation materials. They exhibit good optical and electrical properties. Therefore, they offer promising advantages for different applications. Characteristic features of conducting polymers are due their reversibility and good environmental stability. Presently they are available in market as film which enhance their potentiality for use in many practical applications [61-67].

Polyaniline is a promising polymer because of its unique electrical properties. They polymerise easily and cost of their monomers is low. Therefore, they have wide applications in microelectronic devices, light weight batteries, sensors, super capacitors, microwave absorption and corrosion inhibitor [68-75].

Paper has described preparation of DL-PLA/Cloisite-20A/PANI composite by in-situ technique. Here DL-PLA has been mixed with Cloisite-20A (0.3wt %) solvent. Suitable solvent is used to prepare DL-PLA/Cloisite-20A polymer film. Microstructure, dielectric property, and thermal stability of the prepared composite are evaluated.

## 2. Experimental details

### 2.1. Chemicals and Materials

DL–PLA polymer is procured from Cargill Dow Bair; US–NE. Cloisite 20A and chloroform ($CHCl_3$) are fetched from Merck India.

### 2.2. DL-PLA/Cloisite 20A Nanocomposites Preparation by solution casting process [64-66]

DL-PLA/Cloisite 20A nanocomposite is prepared by solution casting process [76]. In this process, DL-PLA polymer is dissolved with required amount of solvent (i.e., chloroform). To the polymer solution, 4 wt% (with respect to polymer weight) of Cloisite 20A nanoclay is added. DL-PLA polymer solution is stirred for 30 min. This will ensure uniform dispersion of Cloisite 20A nanoclays in DL-PLA polymer solution. Dispersed product is transferred to a petridish where solvent has evaporated out rapidly. There After, DL-PLA/Cloisite 20A nanocomposite film is collected from the petridish. Flow chart of DL-PLA/Cloisite 20A Nanocomposite Preparation is shown in **Figure 1**. The nanocomposite is cut into small pieces for different characterizations.
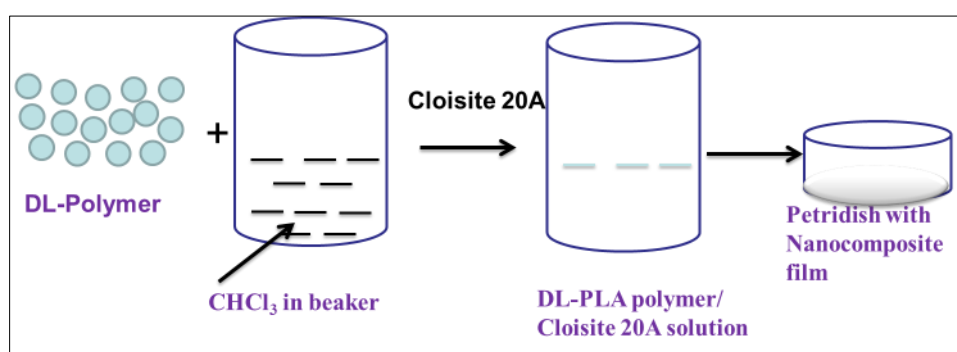


**Figure 1** Flow chart of DL-PLA/Cloisite 20A Nanocomposites Preparation

### 2.3. DL-PLA/Cloisite 20A/PANI Nanocomposites Preparation by in-situ technique

DL-PLA/Cloisite 20A/PANI Nanocomposites is prepared by chemical-oxidation process i.e., *in-situ* method. Liquid aniline is used as conducting polymeric material, whereas DL-PLA/Cloisite 20A film is taken as a base material. The **nanocomposite is prepared at room temperature [64-66]. Three steps involved in the preparation of nanocomposites** by in-situ technique are described below;

#### 2.3.1. Step I Preparation of liquid aniline and DL-PLA/Cloisite 20A films solution

3 mL liquid aniline and DL-PLA/Cloisite 20A films (1.5 cm × 1.5 cm) are put into a 500 mL conical flask containing 105 mL of 1 (M) HCl solution. The solution is stirred (at 600 rpm) for 12 h in a magnetic stirrer. Reaction occurs between soluble aniline and DL-PLA/Cloisite 20A films.

#### 2.3.2. Step II Preparation of Dopant solution

Dopant solution is prepared by taking distilled water and concentrated HCl in appropriate proportion. 7.47 g of ammonium persulphate (oxidant) is added slowly to 60 mL of 1(M) HCl solution. The solution is shacked for shaking (5 minutes).

#### 2.3.3. Step II Preparation of DL-PLA/Cloisite 20A film/PANI Nanocomposites

In this step, prepared oxidant solution is slowly added (i.e., drop wise) to liquid aniline and DL-PLA/Cloisite 20A films mixture solution. Solution is stirred continuously for 10 h. during this period, polymerization reaction proceeds. Color change is noticed from light green to dark green. The nanocomposite is washed with distilled water for several times. After washing, it is followed by drying in air (6 h). Flow-chart for Nanocomposite preparation is shown in Figure 2. Sample from DL-PLA/Cloisite 20A film/PANI Nanocomposite is ready for different tests.
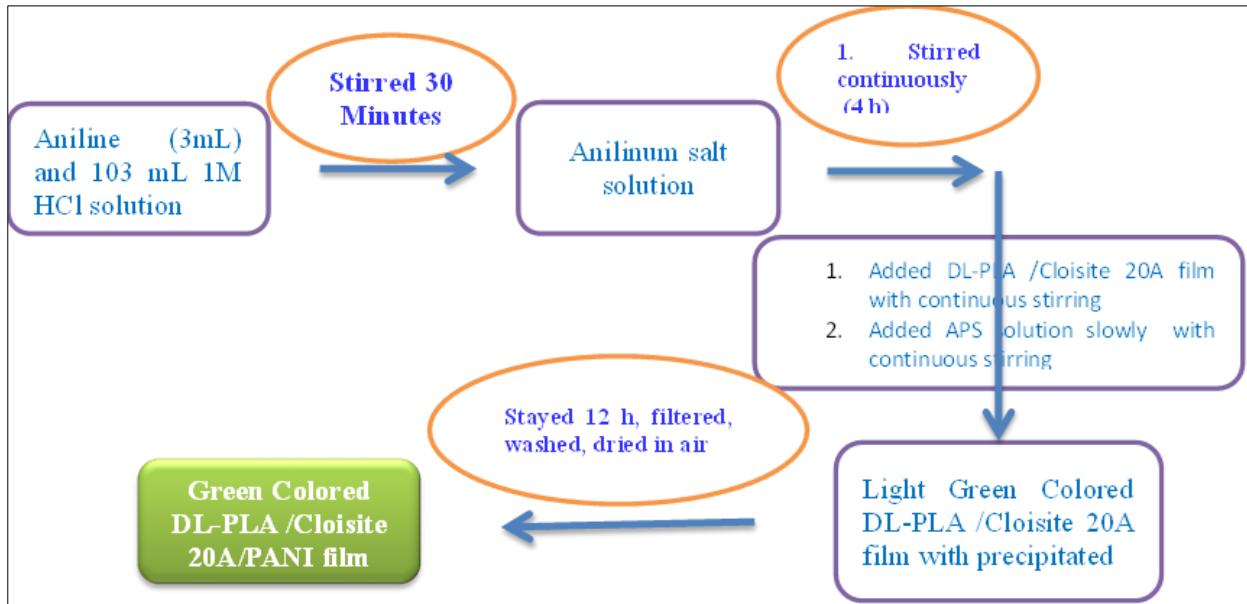
**Figure 2** Flow chart of HCl doped DL-PLA/Cloisite 20A/PANI Film preparation

## 2.4. Characterization techniques

X-ray diffraction (XRD) is made with Phillips PW-1710 advanced wide angle X-ray diffractometer and Phillips PW-1729 X-ray generator. Cu Kα radiation (λ = 0.154 nm) with X-ray generator is maintained at 40 kV and 20 mA.

Fourier transformation infra-red (FTIR) test is done with Thermo Nicolet Nexus 870 spectrophotometer. FTIR spectrum is recorded between 400-4000 cm$^{-1}$. Settings of spectrometer are maintained with 50 scans at 4 cm$^{-1}$ resolution in absorbance mode. Background spectrum is run before taking the FTIR test of the sample.

TGA test of the nanocomposite is done with Perkin Elmer Pyris Diamond analyser. TGA test is performed in Nitrogen environment. In the test, heating rate is maintained to be 10$^{\circ}$/min.

Contact angle is measured on layered substrate which is positioned in sample holder. Distilled water is dropped slowly on the substrate. Silhouette of drop is viewed in a digital camera, attached to a personal computer (PC). Contact angle is estimated through Image analyze software. Attitude is determined 1 second after the drop and is positioned on the substrate surface [67].

AC conductivity is measured by LCR meter. Frequency dependent AC conductivity (σ$_{ac}$) is estimated using the expression [77];

$$\sigma_{ac} = \frac{t \times V_r \cos\left(\frac{\phi}{\pi} \times 180\right)}{RA} \ldots\ldots\ldots\ldots\ldots(2)$$

The following expression is used to estimate dielectric constant (*k*) [77];

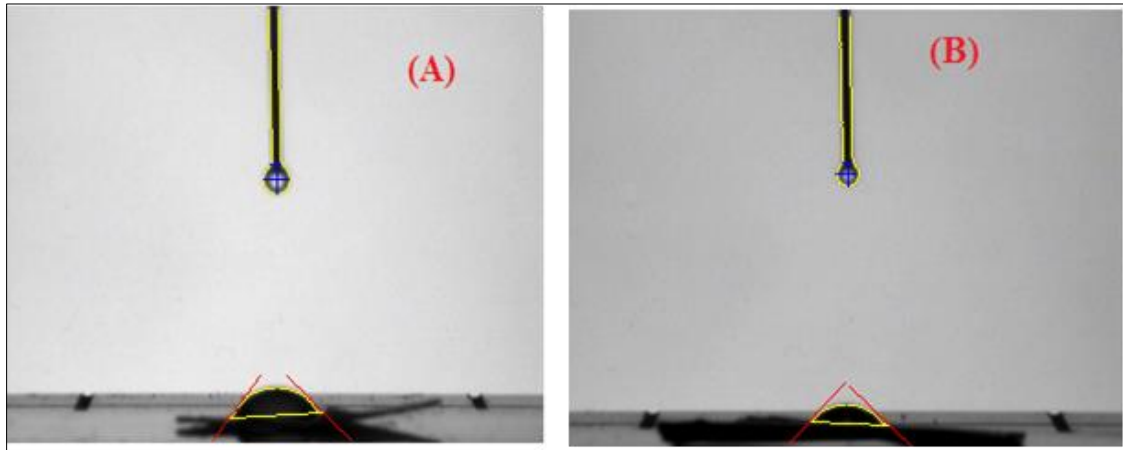$$\varepsilon = \varepsilon_0 \left(\frac{C \times d}{A}\right) \ldots\ldots\ldots\ldots\ldots(2)$$

Here;
$C$ = Capacitance of the pellet
$d$ = Thickness of the pellet (2.5 mm)
$A$ = Cross sectional area of the flat surface of the pellet (100 mm$^2$)
ε$_o$ = Constant of permittivity of free space.

## 3. Results and discussion



**Figure 3** Contact angle/Wettability analyses of DL-PLA (A) and DL-PLA-Cloisite 20A/PANI nanocomposite (B)

Water contact angles are measured to confirm the surface hydrophilicity of the sample. The films hydrophilicity indicates that the sensing film absorbed water drops on the polymeric film surface. The contact angle of water drops on the sensing film surface measured by the sessile drop method [78]. It is well known that the contact angle of a surface is less than 90°, indicates the surface is hydrophilic. **Figure 3** shows Contact angle/Wettability analyses image of DL-PLA (A) and DL-PLA-Cloisite 20A/PANI nanocomposite (B). This study indicates that prepared material is either hydrophilic or hydrophobic nature.

**Table 1** Contact angle of DL-PLA and DL-PLA/Cloisite 20/PANI composite

| S.No. | Sample ID | Contact angle |
|-------|-----------|---------------|
| 1 | DL-PLA | 82.6° |
| **2** | DL-PLA-Cloisite 20A/PANI nanocomposite | 61.2 |
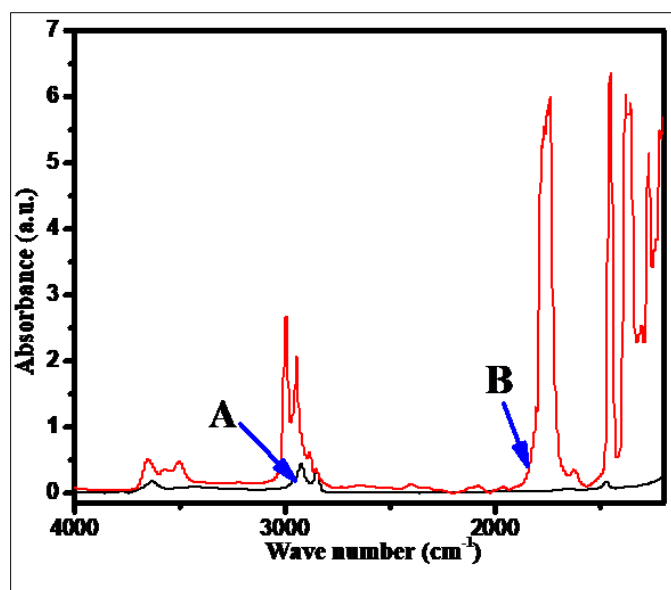


**Figure 4** FTIR plot of Cloisite 20A (A) and DL-PLA/ Cloisite 20A nanocomposite (B)

Analysis is recoded and is mentioned in Table 1. As we can see Table 1, water contact angle for DL-PLA is 82.6° and DL-PLA/Cloisite 20/PANI composite is 61.2°. It is observed that contact angle is lower for DL-PLA/ Cloisite 20/PANI composite. This is attributed to the incorporation of PANI is useful to increase the hydrophillicity and adsorption of water molecules on DL-PLA/ Cloisite 20/PANI composite surface. Increased hydrophilicity has improved water vapor absorption and settling at surface of composite film. An increase in the physisorption process at the sensing film surface enhances sensors sensitivity [67].

Figure 4 displays FTIR spectra of Cloisite 20A (A) and DL-PLA/ Cloisite 20A nanocomposite (B). FTIR spectra show occurrence of different absorption bands which are present in the material. Absorption band ensue at 1117 cm$^{-1}$ wave number is attributed to Si-O band and signifies the occurrence of silicate groups. The absorption bands of DL-PLA at 2995, 1759, 1616 and 1216 cm$^{-1}$ have been attributed to C-H stretching, C=O stretching, C-O stretching of ester and C-O-C stretching vibration, respectively, whereas the bands at 1453, 1361 and 1363 cm$^{-1}$ represent the stretching vibration of C-H deformation of DL-PLA polymer [66, 76]. This indicates that the characteristic absorption features of DL-PLA polymer are retained in the prepared DL-PLA film. The main FTIR bands of PANI-ES are found at 1554, 1475 and 1108 cm$^{-1}$ corresponding to quinoid, benzenoid and C=N stretching, respectively [66, 67, 76]. From our observation, the presence of quinoid and benzenoid ring vibrations are exhibited at 1475 and 1554 cm$^{-1}$ respectively, indicating the presence of oxidation state of PANI-ES. The characteristic band obtained in the ATR-FTIR spectrum of DL-PLA/PANI-ES composite film indicates the formation of conducting DL-PLA/PANI-ES composite films. It is observed that N-H bands of HCl doped DL-PLA/PANI-ES appeared at 3289. The entire bands indicate that both PANI-ES and DL-PLA are retained in the composites.
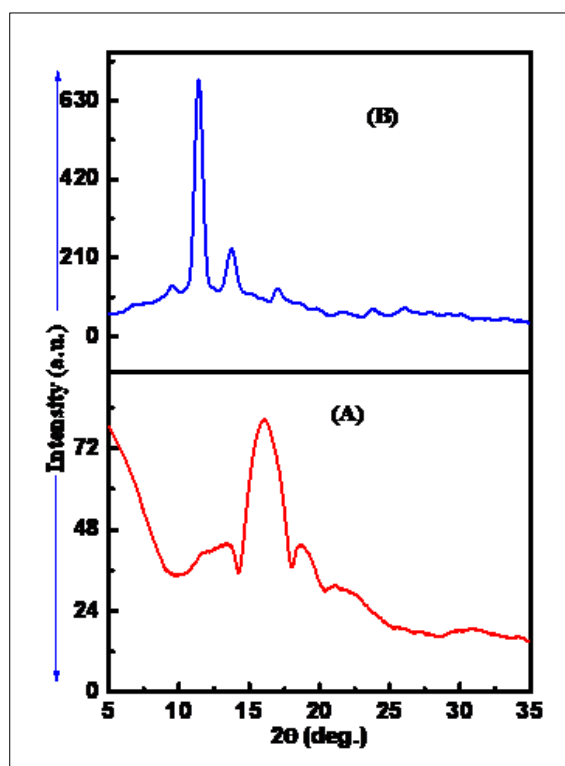


**Figure 5** XRD plot of DL-PLA (A) and DL-PLA/ Cloisite 20A nanocomposite (B)

Diffraction pattern is shown in Figure 5. Figure 5A shows absence any sharp peaks indicating amorphous nature of the material. However, there is a broaden peak shown near 15$^0$ (Figure 5A). Diffraction pattern of composite is shown in Figure 5B. Here, the pattern has marked difference observed in the diffraction pattern of Figure 5B if it is compared with diffraction pattern observed in Figure 5A. There is a narrow sharp peak observed around 11-12$^0$ followed by another peak near to 15$^0$. Additionally, occurrences of small peaks are seen in the other Bragg's angels. Therefore, composite materials have shown presence of crystalline phases in the composite materials. These results, correlate with the findings of enhanced degree of crystallinity of DL-PLA/Cloisite 20A/PANI Composite which is attributed to the transcrystaline of the polymer due to addition of PANI in DL-PLA polymer. Thus, this will improve thermal resistance of composite which is proven by its higher crystallite with denser lamella [78-80].
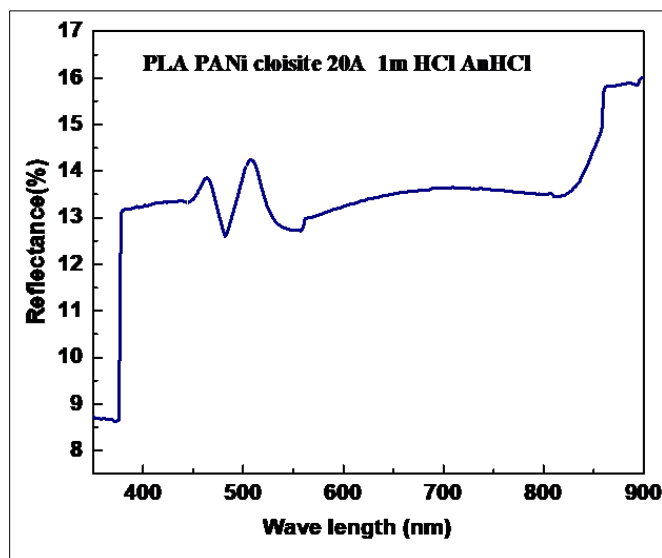
**Figure 6** UV Visible plot of DL-PLA/ Cloisite 20A nanocomposite

It is found from literature that PANI-ES shows $\pi$-$\pi^*$ transition (of benzoid ring), polaron to $\pi^*$, benzoid to quinoid ring, and polaron transition [64-66]. However, no transition is observed for DL-PLA polymer flim [64-66]. Different transitions are observed in DL-PLA/Cloisite 20A/PANI Composite (Vide-Figure 6). In the composite, two types of bands such as $\pi$ to localized polaron band   and $\pi$-$\pi^*$(of benzoid ring) are found. Both transitions suggest presence of anilinic unit and oxidation unit in emeradlline salt form of composite flim [64-66]. Thus, there is indication of conjugation length affecting band gap energy. Hence, electrons are delocalized in the excitation band.
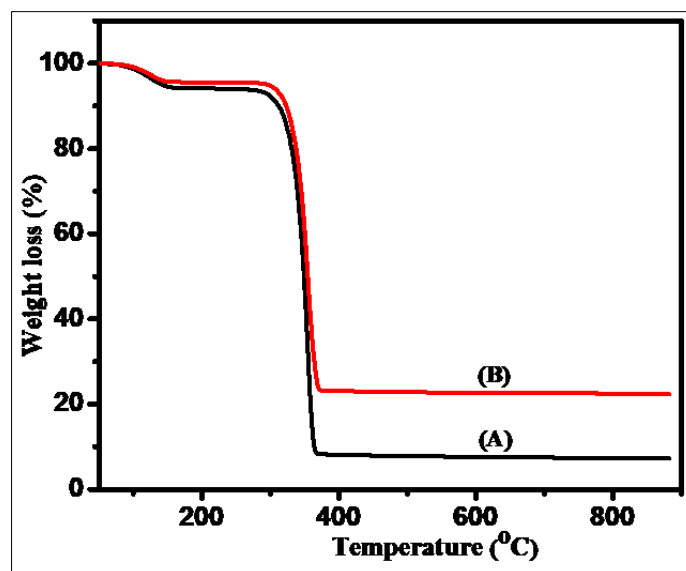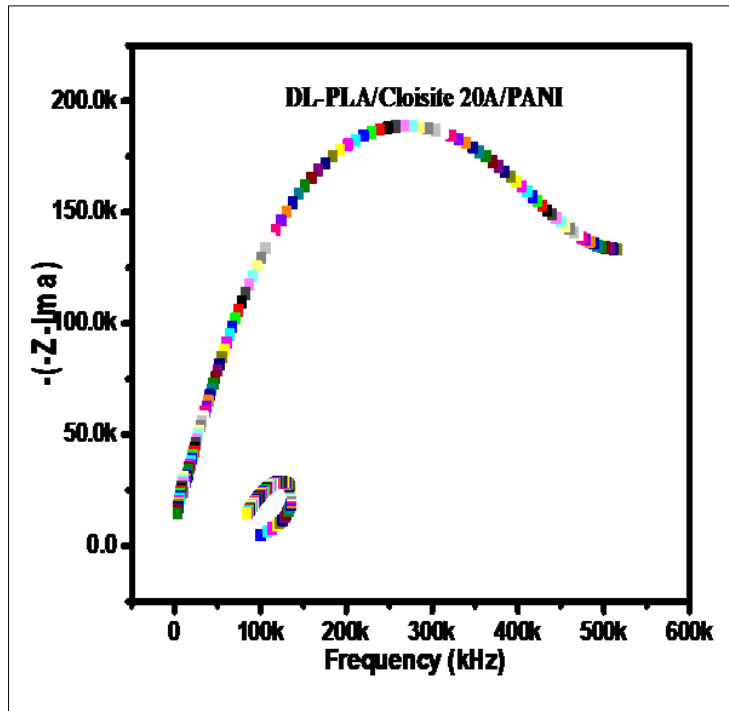


**Figure 7** TGA plot of DL-PLA (A) and DL-PLA/ Cloisite 20A/PANI nanocomposite (B)

Figure 7 shows TGA analyses of DL-PLA (A) and DL-PLA/Cloisite 20A/PANI Composite (B). For plotting the graph, weight loss has been established at different temperatures ranging between 30-800 $^0$C. Data plot is depicted in Figure 7 as weight loss *vs* temperature. Between 75-100 $^0$C, there is a slight loss in weight. Thereafter, weights remain same till 350 $^0$C. Beyond 350 $^0$C, weights loss further for both the materials have dropped sharply.  There is a change in weight further I both the materials (mentioned Figure 7) beyond 350 $^0$C.  First stage weight loss is attributed to loss of water molecules occurring in the surface of the materials. Second stage weight loss indicates decomposition of the materials and its composite [81].

**Figure 8** [- (-Z img)] vs frequency plot of DL-PLA/ Cloisite 20A nanocomposite

PANI based composite has a mixed electronic–ionic exchange condition at the film /electrolyte or dopant interface [82, 83]. Electronic charge transfers through the electrodes at the DL-PLA/Cloisite 20A film surface. Ions of electrolyte move also ingress/outgress freely at both interfaces. Charge conduction in DL-PLA/Cloisite 20A/PANI composite film surface is electronic–ionic in nature. This takes by polaron/bi-polaron transition of PANI structures involving anion hoping along and across the chains [84, 85].

**Figure** 8 shows ES results of PANI in DL-PLA/ Cloisite 20A/ PANI composite in Nyquist format where the imaginary component of impedance (–Z") is plotted against the real component (Z') as a function of frequency. In **Figure** 8, semicircle represents the response of an equivalent electrical circuit (i.e., parallel combination of R–C (resistor–capacitor). the Relaxation in the combination is signified by a characteristics time of RC. It characterizes the first order transition in charge of conduction processes. The impedance represents a pure resistance at both extreme frequency at f = 0 and f =∞. Here, 'f' is the linear frequency (Hz). The peak in Z" is observed at the characteristic frequency (ω*, radians/s). The characteristic frequency (ω*) is expressed as [86];

$$\omega^8 = \frac{1}{2\pi f} = \tau = \frac{1}{RC} \ldots\ldots\ldots\ldots\ldots\ldots(3)$$

Here, f* is the characteristic linear frequency (Hz). In low frequency range, it shows impedance resolution. This indicates diffusionally controlled slow charge transport processes [87-89]. The large values of impedance are due to the insulating nature of the materials. The low-frequency impedance can be assigned to slow charge transfer at the interface.

Relaxation in the charge transfer processes cannot be represented by a single time constant. This is due to composite nature of the film and non-uniform surfaces. The capacitance is spatially distributed and is evidenced by a depressed semicircle in the **Nyquist plot.** In this case, distributed capacitance is represented by a constant phase element (Q) for which the impedance is expressed as:

$$Z\ (j\omega) = \frac{1}{Y_0}(j\omega)^{-\alpha} \ldots\ldots\ldots\ldots\ldots(4)$$

Here, $Y_0$ represents the admittance (i.e., 1/Z)

Q represents capacitance dispersion index of the constant phase element
The Q value varies between −1 and +1.
Q value of a pure conductance = −1, resistance ₌ = 0 and capacitance = 1.

First R–Q loop represents charge transport process in bulk material that involves a charge transfer resistance in the composite film phase and a double layer capacitance of electrolyte [90-92]. The second R–Q loop represents slow transfer processes which occur along the whole thickness of composite. For the composite, it may indicate the absorption of a doping anion (Cl−) at the surface and subsequent passage through the composite via most probable polaron–bipolaron transition [90, 93, 94]. The low-frequency asymptotic limit of the impedance of the composite synthesized using two-compartment cell represents ohmic current at electrodes and hence R2 is a sum of electronic and ionic resistance of the composite film [90-94]. The relative contribution of electronic and ionic transport depends on the conductivity of the composite determined by the extent of PANI deposition in the composite film. In this case, resistance of second loop may be attributed to the resistance of redox reactions in PANI involving an adsorption process at the composite film surface. Low resistance values of both high and low frequency semicircles shows presence of conductive PANI phase in the composite. High capacitance values coupled with low resistance of low frequency semicircle indicates typical pseudocapacitance of doped PANI [95, 96]. This may be attributed to the absorption and diffusion of charge carrying through a thick and dense surface PANI layer. The insufficient retention of electrolyte may offer a significant resistance to diffusing ions through thick PANI layer and as a result, impedance curve does not intersect real impedance axis indicating very slow (highly hindered) diffusion through the composite film.

Relaxation process at low frequencies has been assigned to the pseudocapacitance arising from the charge transport processes in PANI phase [97-99]. A typical value of ~0.5 F of the low frequency capacitance has already been observed for HCl doped PANI film and is assigned to the pseudocapacitance of interfacial charge transfer [95, 96]. Charge transfer processes in PANI involve H+/anion coupled transport where anions are free to move along with the protonated imine sites in PANI [100].
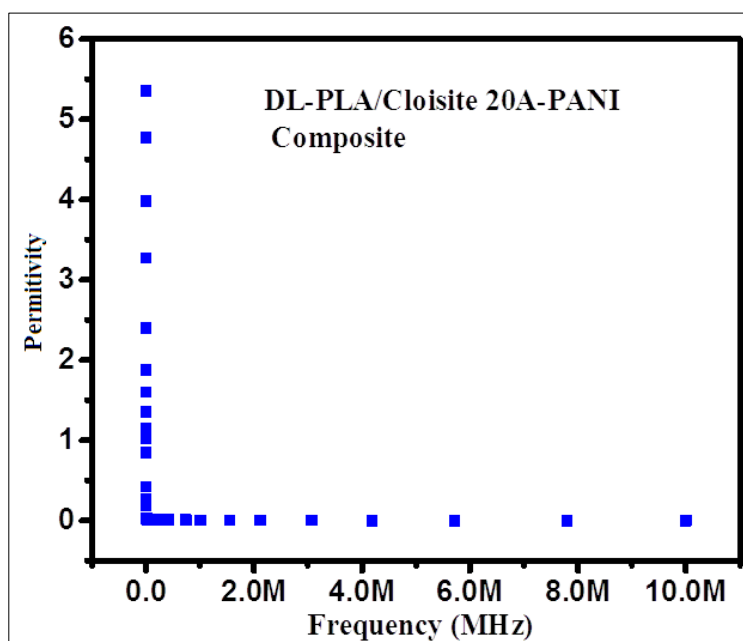


**Figure 9** Permittivity of DL-PLA/ Cloisite 20A-PANI Composite

Figure 9 displays variation of frequency dependence of permittivity value (or dielectric constant ($\varepsilon$)) and dielectric loss of DL-PLA/ Cloisite 20A-PANI Composite. Dielectric permittivity of the Composite measured from 0.1 MHz to 10MHz at room temperatures. From Figure 9, it is seen that dielectric constant is decreased at low frequency region and then is constant with increasing the frequency. This is due to the effect of field and/or tightly pinned to the polymer chain [101, 102]. At low frequency region, the permanent dipoles align themselves along the field and contribute fully to the total polarization of the dielectric. At higher frequency region, the variation in the field is very rapid for the dipoles to align themselves, so their contribution to the polarization and hence, to dielectric permittivity can become negligible. Therefore, the dielectric permittivity, $\varepsilon'$ decreases with increasing frequency. Decrease of dielectric constant $\varepsilon'$ can be explained from interfacial polarization. Interfacial polarization arises as a result of difference in conducting phase, but

is interrupted at grain boundary due to lower conductivity. Generally in polycrystalline materials, the grains exhibit semi conducting behavior while the grain boundary are insulators. The maximum in the ε'' peak shifts towards higher frequency region as the temperature increases indicating a thermally activated process. Variation of permittivity with frequency is related to the applied field that assists electron hopping between two different sites of the materials. At higher frequency region, the charge carriers will no longer be able to rotate rapidly, so their oscillation will begin to lay behind this field resulting in a decrease of dielectric permittivity, ε'. It is observed that dielectric constant ε' is reduced rapidly at lower frequencies and shows almost frequency independent behavior at higher frequency region.
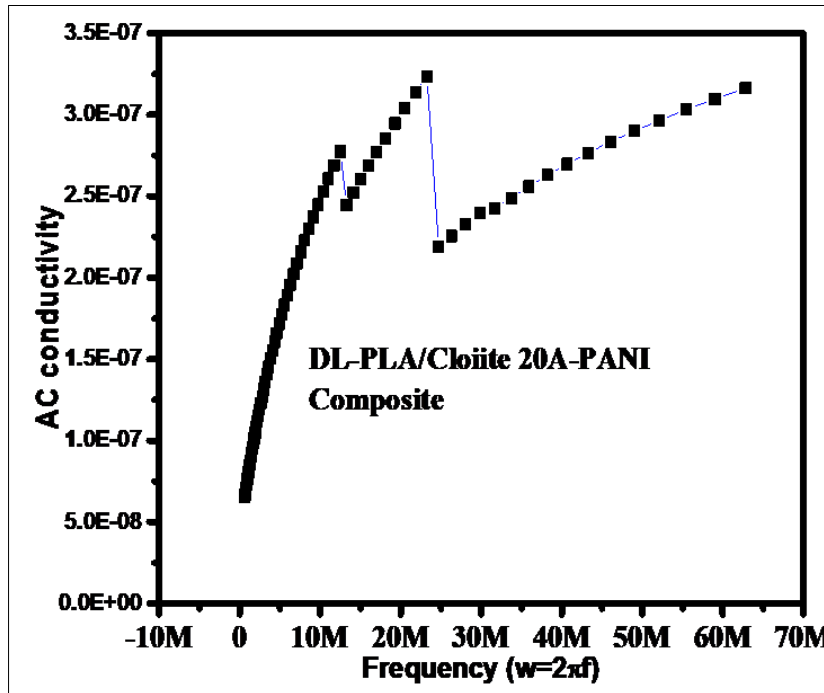


**Figure 10** AC-conductivity of DL-PLA/ Cloisite 20A-PANI Composite

Electrical conductivity measurements are closely related to electronic properties of materials. In composites, an AC conductivity measurement provides useful information relating to relaxation phenomenon and co-relate with electrical polarization process. Figure 11 shows AC conductivity of DL-PLA/Cloisite 20A-PANI Composite at different frequencies. Frequency dependency (0.1 MHz-10 MHz) AC conductivity of DL-PLA/Cloisite 20A-PANI Composite at room temperatures is depicted in Figure 11. Expression of AC electrical conductivity ($\sigma_{ac}$) is a non-linearly function of dielectric permittivity ($\varepsilon i$) and angular frequency ($\omega = 2\pi F$). The relation is followed as in Equation 5 [77, 103-106];

$$\sigma_{AC} = \omega\varepsilon_0\varepsilon_i \ldots\ldots\ldots\ldots\ldots\ldots(5)$$

Samples under testing, $\sigma_{ac}$ increases with increasing frequency. This trend is in good agreement with reported polymers and polymers composite materials. This is due to small polaron hopping in the polymer backbone [104].

## 4. Conclusion

DL-PLA/Cloisite 20A nanocomposite is prepared by adopting solution technique route, whereas DL-PLA/Cloisite 20A/PANI nanocomposite is successfully synthesized. 3 wt% Cloisite 20A has exhibited higher thermal stability in comparison to DL-PLA polymer and PANI-ES polymer. XRD, FTIR, and UV Visible results have confirmed deposition of polyaniline polymer on the surface of DL-PLA/Cloisite 20A film via covalent bonding. AC electrical conductivity is described as a function of frequency. The nanocomposite shows low value of AC conductivity. Developed biodegradable PLA nanocomposite with low dielectric loss may pave a way to disposable electronics. Combined effect of DL-PLA polymer and Cloisite 20A has reduced direct contact and thereby, increase the distance between matrix materials. This has resulted in low dielectric loss. Addition of Cloisite 20A can serve as nucleation sites to improve crystallinity of PLA without affecting crystal phase. Crystallinity of PLA/ Cloisite 20A/PANI nanocomposite is increased due to presence of PANI polymer.

## Compliance with ethical standards

*Disclosure of conflict of interest*

No conflict of interest to be disclosed.

## References

[1] H. K. Dietz, (2006), Fine lines in high yield (Part CXXIV): high performance dielectrics. CircuiTree, Vol. 19(1), pp. 52–53.

[2] C. J. Dias and D. K. Das-Gupta, (1996), Inorganic ceramic/polymer ferroelectric composite electrets, IEEE Transactions on Dielectrics and Electrical Insulation, Vol. 3(5), pp. 706–734.

[3] E. Reichmanis, H. Katz, C. Kloc, and A. Maliakal, (2005), Plastic electronic devices: from materials design to device applications, Bell labs technical journal, Vol. 10(3), pp. 87–105.

[4] Rao, Y., Yue, J. and Wong, C. P., (2001), High K polymer-ceramic nano-composite development, characterization, and modeling for embedded capacitor RF application, IEEE Conference Proceedings of Electronic Components and Technology, pp. 1408–1412.

[5] D. H. Kuo, C. C. Chang, T. Y. Su, W. K. Wang, and B. Y. Lin, (2004), Dielectric properties of three ceramic/epoxy composites, Materials Chemistry and Physics, Vol. 85, pp. 201–206.

[6] S. D. Cho, K. W. Jan, J. G. Hyun, S. Lee, K. W. Paik, and H. Kim, (2005), Epoxy/$BaTiO_3$ composite films and pastes for high dielectric constant and low-tolerance embedded capacitors fabrication in organic substrates, IEEE Transactions on Components, Packaging and Manufacturing Technology, Vol. 28(4), pp. 297–303.

[7] Y. Rao, A. Takahashi, and C. P. Wong, (2003), Di-block copolymer surfactant study to optimize filler dispersion in high dielectric constant polymer–ceramic composite, Composite Part A, Vol. 34, pp. 1113–1116.

[8] L. Ramajo, M. Reboredo, and M. Castro, (2005), Dielectric response and relaxation phenomena in composites of epoxy resin with $BaTiO_3$ particles, Composite Part A, Vol. 36, pp. 1267–1274.

[9] C. Muralidhar and P. K. C. Pillai, (1987), Dielectric behaviour of barium titanate ($BaTiO_3$)/polyvinylidene fluoride (PVDF) composite, Journals of Materials. Science Letter, Vol. 6, pp. 346–348.

[10] S. U. Adkary, H. L. W. Chan, C. L. Choy, B. Sundaravel, and I. H. Wilson, (2002), Characterisation of proton irradiated $Ba_{0.65}Sr_{0.35}TiO_3$/P(VDF-TrFE) ceramic-polymer composites, Composite Science and Technology, Vol. 62, pp. 2161–2167.

[11] J. W. Liou, and B. S. Chiou, (1998), Dielectric tunability of barium strontium titanate/silicone-rubber composite, Journal of Physics and Condensed Matter, 1998, Vol. 10, pp. 2773–2786.

[12] S. H. Xie, X. Z. Wei, Z. K. Xu, and Y. Y. Xu, (2005), Polyimide/$BaTiO_3$ composites with controllable dielectric properties, Composite Part A, Vol. 36, pp. 1152–1157.

[13] M. Olszowy, Cz. Pawlaczyk, E. Markiewicz, and J. Kulek, (2005), Dielectric and pyroelectric properties of BaTiO3-PVC composites, Physica Status Solidi (a), Vol. 202(9), pp. 1848–1853.

[14] C. K. Chiang and R. Popielarz, (2002), Polymer composites with high dielectric constant, Ferroelectrics, Vol. 275, pp. 1–9.

[15] P. Badheka, V. Magadala, N. G. Devaraju, B. I. Lee, and E. S. Kim, (2006), Effect of dehydroxylation of hydrothermal barium titanate on dielectric properties in polystyrene composite. Journal of Applied Polymer Science, Vol. 99, pp. 2815–2821.

[16] S. M. Abbas, M. Chandra, A. Verma, R. Chatterjee, and T. C. Goel, (2006), Complex permittivity and microwave absorption properties of a composite dielectric absorber, Composite Part A, Vol. 37, pp. 2148–2154.

[17] Y. Wang and J. Huang, (1996), Single screw extrusion compounding of particulate filled thermoplastics: state of dispersion and its influence on impact properties, Journal of Applied Polymer Science, Vol. 60, pp. 1779–1791.

[18] S. Bahadur and C. Sunkara, (.2005), Effect of transfer film structure, composition and bonding on the tribological behaviour of polyphenylene sulfide, Wear, Vol. 258, pp. 1411-1421

[19] M. K. Panigrahi, N. K. Singh, R. M. Banik, Pralay Maiti, (2010), Improved Biodegradation and Thermal Properties of Poly (Lactic Acid)/Layered Silicate Nanocomposites, Composite interface 17(2010)143–158.

[20] Z. B. Li, B. H. Tan, T. T. Lin and C. B. He (2016), Recent advances in stereocomplexation of enantiomeric PLA-based copolymers and applications, Progress in Polymer Science, Vol. 62, pp. 22–72.

[21] W. Wu, S. T. Han, S. Venkatesh, Q. J. Sun, H. Y. Peng, and Y. Zhou, (2018), Biodegradable skininspired nonvolatile resistive switching memory based on gold nanoparticles embedded alkali lignin, Organic Electronics, Vol. 59, pp. 382–8.

[22] X. W. Shi, X. Dai, Y. Cao, J. W. Li, C. G. Huo, and X. L. Wang. (2017), Degradable poly(lactic acid)/metalorganic framework nanocomposites exhibiting good mechanical, flame retardant, and dielectric properties for the fabrication of disposable electronics, Industrial & engineering chemistry research, Vol. 56(14), pp. 3887–94.

[23] X. H. Wu, Y. Ma, G. Q. Zhang, Y. L. Chu, J. Du, and Y. Zhang, (2015), Thermally stable, biocompatible, and flexible organic field-effect transistors and their application in temperature sensing arrays for artificial skin, Advanced Functional Materials, Vol. 25(14), pp. 2138–46.

[24] W. Yang, B. Tawiah, C. Yu, Y. F. Qian, L. L. Wang, and A. C. Y. Yuen, (2018), Manufacturing, mechanical and flame retardant properties of poly (lactic acid) biocomposites based on calcium magnesium phytate and carbon nanotubes, Composites Part A: Applied Science, Vol. 110, pp. 227–36.

[25] W. Wu, X. W. Cao, Y. J. Zhang, G. J He, (2013), Polylactide/halloysite nanotube nanocomposites: thermal, mechanical properties, and foam processing, Journal of Applied Polymer Science, Vol. 130(1), pp. 443–52.

[26] W. Yang, W. J. Yang, B. Tawiah, Y. Zhang, L. L. Wang, S. E. Zhu, (2018), Synthesis of anhydrous manganese hypophosphite microtubes for simultaneous flame retardant and mechanical enhancement on poly (lactic acid), Composite Science and Technology, Vol. 164, pp. 44–50.

[27] J. D. Badia, P. Reig-Rodrigo, R. Teruel-Juanes, T. Kittikorn, E. Stromberg, and M. Ek, (2017), Effect of sisal and hydrothermal ageing on the dielectric behaviour of polylactide/sisal biocomposites, Composite Science and Technology, Vol. 149, pp. 1–10.

[28] U. Sonchaeng, F. Iñiguez-Franco, R. Auras, S. Selke, M. Rubino, and L.T. Lim, (2018), Poly(lactic acid) mass transfer properties, Progress in Polymer Science, Vol. 86, pp. 85–121.

[29] W. J. Barrier Koros, (1990), Polymers and Structures, Analytical Chemistry, Vol. 62, pp. 737A-xxx.

[30] M. S. Hedenqvist, Barrier packaging materials. In Handbook of Environmental Degradation of Materials, 3rd ed.; Kutz, M., Ed.; Elsevier Inc.: Cambridge, MA, USA, 2018.

[31] K. Majeed, M. Jawaid, A. Hassan, A. Abu Bakar, H .P. S. Abdul Khalil, A. A. Salema, and I. Inuwa, (2013), Potential materials for food packaging from nanoclay/natural fibres filled hybrid composites, Materials & Design, Vol. 46, pp. 391–410.

[32] S. L. Bee, M. A. A. Abdullah, S. T. Bee, L. T. Sin, and A.R. Rahmat, (2018), Polymer nanocomposites based on silylated-montmorillonite: A review, Progress in Polymer Science, Vol. 85, pp. 57–82.

[33] C. Silvestre, D. Duraccio, and S. Cimmino, (2011), Food packaging based on polymer nanomaterials, Progress in Polymer Science, Vol. 36, pp. 1766–1782.

[34] S. Sinha Ray, and M. Okamoto, (2003), Polymer/layered silicate nanocomposites: A iiiiiiiiireview from preparation to processing, Progress in Polymer Science, Vol. 28, pp. 1539–i1641.

[35] D. Nordqvist, and M. S. Hedenqvist, Transport Properties of Nanocomposites Based on iPolymers and Layered Inorganic Fillers. In Packaging Nanotechnology; Mohanty, A.K., iMisra, M., Eds.; American Scientific Publishers: Valencia, CA, USA, 2009.

[36] O. C. Wokadala, S. S. Ray, J. Bandyopadhyay, J. Wesley-Smith, and N. M. Emmambux, i(2015), Morphology, thermal properties and crystallization kinetics of ternary blends of tihe polylactide and starch biopolymers and nanoclay: The role of nanoclay hydrophobicity, Polymer, Vol. 71, pp. 82–92.

[37] W. H. Hoidy, E. A. J. ;Al-Mulla, and K. W. Al-Janabi, (2010), Mechanical and Thermal Properties of PLLA/PCL Modified Clay Nanocomposites, Journal of Polymers and the Environment, Vol. 18, pp. 608–616.

[38] Ibrahim, N.; Jollands, M.; Parthasarathy, R. (2017), Mechanical and thermal properties of melt processed PLA/organoclay nanocomposites, IOP Conference Series of Materials Science & Engineering, Vol. 191, pp. 012005-xxx.

[39] P. Krishnamachari, J. Zhang, J. Lou, J. Yan, and L. Uitenham, (2009), Biodegradable poly(Lactic Acid)/clay nanocomposites by melt intercalation: A study of morphological, thermal, and mechanical properties, International Journal of Polymer and Analytical Characterization, 2009, Vol. 14, pp. 336–350.

[40] A. Hasook, S. Tanoue, Y. Iemoto, and T. Unryu, (2006), Characterization and mechanical properties of poly(lactic acid)/poly(_-caprolactone)/organoclay nanocomposites prepared by melt compounding, Polymer Engineering Science, Vol. 46, pp. 1001–1007.

[41] S. M. Lai, S. H. Wu, G. G. Lin, and T. M. Don, (2014), Unusual mechanical properties of melt-blended poly(lactic acid) (PLA)/clay nanocomposites, European Polymer Journal, Vol. 52, pp. 193–206.

[42] S. H. Tabatabaei and A. Ajji, (2011), Orientation, mechanical, and optical properties of poly (lactic acid) nanoclays composite films, Polymer Engineering Science, Vol. 51, pp. 2151–2158.

[43] H. M. Cele, V. Ojijo, H. Chen, S. Kumar, K. Land, T. Joubert, M. F. R. De Villiers, and S. S. Ray, (2014), Effect of nanoclays on optical properties of PLA/clay composite films Polymer Testing, Vol. 36, pp. 24–31.

[44] P. Stloukal, S. Pekaˇrová, A. Kalendova, H. Mattausch, S. Laske, C. Holzer, L. Chitu, S. Bodner, G. Maier, and M. Slouf, (2015), Kinetics and mechanism of the biodegradation of PLA/clay nanocomposites during thermophilic phase of composting process, Waste Management, Vol. 42, pp. 31–40.

[45] E. Castro-Aguirre, R. Auras, S. Selke, M. Rubino, and T. Marsh, (2018), Impact of nanoclays on the biodegradation of poly(lactic acid) nanocomposites, Polymers, Vol. 10, pp. 202-xxx.

[46] C. Rovera, M. Ghaani, and S. Farris, (2020), Nano-inspired oxygen barrier coatings for food packaging applications: An overview, Trends in Food Science and Technology, Vol. 97, pp. 210–220.

[47] G. Choudalakis and A. D. Gotsis, (2009), Permeability of polymer/clay nanocomposites: A review, European Polymer Journal, Vol. 45, pp. 967–984.

[48] M. Kotal and A. K. Bhowmick, (2015), Polymer nanocomposites from modified clays: Recent advances and challenges, Progress Polymer Science, Vol. 51, pp. 127–187.

[49] T. T. Zhu, C. H. Zhou, F. B. Kabwe, Q. Q. Wu, C. S. Li, and J. R. Zhang, (2019), Exfoliation of montmorillonite and related properties of clay/polymer nanocomposites, Applied Clay Science, Vol. 169, pp. 48–66.

[50] B. Tan and N. L. Thomas, (2016), A review of the water barrier properties of polymer/clay and polymer/grapheme nanocomposites, Journal of Membrane Science, Vol. 514, pp. 595–612.

[51] C. Wolf, H. Angellier-Coussy, N. Gontard, F. Doghieri, and V. Guillard, (2018), How the shape of fillers affects the barrier properties of polymer/non-porous particles nanocomposites, A Review  Journal of Membrane Science, Vol. 556, pp. 393–418.

[52] A. Kalendova, D. Merinska, J. F. Gerard, and M. Slouf, (2013), Polymer/clay nanocomposites and their gas barrier properties, Polymer Composite, Vol. 34, pp. 1418–1424.

[53] Y. Cui, S. Kumar, Rao B. Kona, and D. Van Houcke, (2015), Gas barrier properties of polymer/clay nanocomposites, RSC Advance, Vol. 5, pp. 63669–63690.

[54] J. M. Raquez, Y. Habibi, M. Murariu, and P. Dubois, (2013), Polylactide (PLA)-based nanocomposites, Progress in Polymer Science, Vol. 38, pp. 1504–1542.

[55] Z. M. Dang, L. Wang, Y. Yin, Q. Zhang, Q. Q. Lei, (2007), Giant dielectric permittivities in functionalized carbon-nanotube/electroactive-polymer nanocomposites, Advanced Materials, Vol. 19, pp. 852–7.

[56] J. M. Zhu, X. Y. Ji, M. Yin, S. Y. Guo, and J. B. Shen, (2017), Poly (vinylidene fluoride) based percolative dielectrics with tunable coating of polydopamine on carbon nanotubes: Toward high permittivity and low dielectric loss, Composite Science and Technology, Vol. 144, pp. 79–88.

[57] Y. Gao, C. Z. Wang, J. Li, and S. Y. Guo,  (2019), Adjustment of dielectric permittivity and loss of graphene/thermoplastic polyurethane flexible foam: Towards high microwave absorbing performance, Composite Part A: Applied Science, Vol. 117, pp. 65–75.

[58] X. J. Zha, J. H. Pu, L. F. Ma, T. Li, R. Y. Bao, and L. Bai L,(2018), A particular interfacial strategy in PVDF/OBC/MWCNT nanocomposites for high dielectric performance and electromagnetic interference shielding. Composite Part A: Applied Science, Vol. 105, pp. 118–25.

[59] M. H. Yang, H. Zhao, D. L. He, J. B. Bai, (2017), Constructing a continuous amorphous carbon interlayer to enhance dielectric performance of carbon nanotubes/polyvinylidene fluoride nanocomposites, Carbon, Vol. 116, pp. 94–102.

[60] T. Maharana, B. Mohanty, and Y. S. Negi, (2009), Melt-solid polycondensation of lactic acid and its biodegradability, Progress in Polymer Science, Vol. 34, pp. 99–124.

[61] V. Krikorian and D. J. Pochan, (2003), Poly (l-Lactic Acid)/Layered Silicate Nanocomposite: Fabrication, Characterization, and Properties, Chemistry of Materials, Vol. 15, pp. 4317–4324.

[62] G. B. Shumaila, V. S. Lakshmi, M. Alam, A. M. Siddiqui, M. Zulfequar and M. Husain, (2010), Synthesis and Characterization of Se doped Polyaniline, Current Applied Physics, Vol. 11 pp. 217-222.

[63] Safenaz M. Reda, Sheikha M. Al-Ghannam, (2012), Synthesis and electrical properties of Polyaniline nanocomposites with silver nanoparticles, Advances in Materials Physics and Chemistry, Vol. 2, pp. 75-81.

[64] M. K. Panigrahi and B. Adhikari, (2021), Cloisite 20A based Polyaniline Nanocomposites for Nitrogen Dioxide (NO$_2$) Gas Sensors, Book Chapter, ISBN: 9789390853403, DOI:10.34256/ioriip2123, IOR PRESS.

[65] M. K. Panigrahi and B. Adhikari, (2021), Acrylic Acid (AA) based Polyaniline Composite for Liquefied Petroleum Gas (LPG) Sensors, Book Chapter, ISBN: 9789390853403, DOI: 10.34256/ioriip2124, IOR PRESS.

[66] M. K. Panigrahi and B. Adhikari, (2021), DL-Polylactide (DL-PLA) Based Polyaniline Composite For Hydrogen Gas Sensors, Book Chapter, ISBN: 9789390853403, DOI: 10.34256/ioriip2125, IOR PRESS.

[67] M. K. Panigrahi, (2022), Investigation of Wettability and Ac-Conductivity of EVA/PANI-ES Composite, Bulletin of Scientific Research, Vol. 4(2), pp. 15-23.

[68] M. Bahmanyar, S. Sedaghat, A. Ramazani S.A., H. Baniasadi, (2015), Preparation of Ethylene Vinyl Acetate Copolymer/ Graphene Oxide Nanocomposite Films via Solution Casting Method and Determination of the Mechanical Properties, Polymer-Plastics Technology and Engineering, Vol. 54, pp. 218–222.

[69] I. Fratoddi, I. Venditti, C. Cametti, and M. V. Russo (2015), Chemiresistive polyaniline-based gas sensors: A mini review, Sensors and Actuators B: Chemical, Vol. 220, pp. 534-548.

[70] B. D. Malhotra, Asha Chaubey, and S. P. Singh (2006) Prospects of conducting polymers in biosensors, Analytica Chimica Acta, Vol. 578, pp. 59–74.

[71] Ryu, K. S., Kim, K. M., Kang, S. G., Lee, G. J., Joo, J., and Chang, S. H. (2000), Electrochemical and physical characterization of lithium ionic salt doped polyaniline as a polymer electrode of lithium secondary battery, Synthetic Metals, Vol. 3, pp. 213–217.

[72] S. Sathiyanarayanan, S. K. Dhawan, D. C. Trivedi, and K. Balakrishnan, (1992), Soluble conducting poly ethoxy aniline as an inhibitor for iron in HC1, Corrosion Science, Vol. 33, pp. 1831–1841.

[73] R. H. Baughman, (1996), Conducting polymer artificial muscles, Synthetic Metals, Vol. 78, pp. 339–353.

[74] E. Frackowiak, V. Khomenko, K. Jurewicz, K. Lota, and F. Be'guin (2006), Supercapacitors based on conducting polymers/nanotubes composites, Journal of Power Sources, Vol. 153, pp. 413–418.

[75] J. H. Burroughes, D. D. C. Bradley, A. R. Brownn, R. N. Marks, K. Mackay, R. H. Friend, P. L. Burns, and A. B. Homes, (1990), Light–emitting diodes based on conjugated polymers, Nature, Vol. 347, pp. 539–541.

[76] A. Ohtani, M. Abe, M. Ezoe, T. Doi, T. Miyata, and A. Miyake, (1993), Synthesis and properties of high molecular weight soluble polyaniline and its application to the 4 MB–capacity barium ferrite floppy disk's antistatic coating, Synthetic Metals, Vol. 57, pp. 3696–3701.

[77] M. K. Panigrahi, N. K. Singh, R. K. Gautam, R. M. Banik, and P. Maiti, (2010), Improved Biodegradation and Thermal Properties of Poly(lactic acid)/Layered Silicate Nanocomposites, Composite Interfaces, Vol. 17, pp. 143–158.

[78] H. M. Zeyada, F. M. El-Taweel, M. M. El-Nahass, and M. M. ElShabaan, (2016), Effect of substitution group on dielectric properties of 4H-pyrano [3, 2-c] quinoline derivatives thin films, Chinese Physics B, Vol. 25, pp. 1-8.

[79] J. G. Alonso, C. Dalmolin, J. Nahorny, A. A.C. Recco, L. C. Fontana, and D. Becker, (2018), Active screen plasma system applied to polymer surface modification: poly(lactic acid) surface activation before polyaniline graft polymerization in aqueous medium, Journal of polymer Engineering, Vol. xxx, pp.1-8.

[80] X. Wang, Y. Tang, X. Zhu, Y. Zhou, X. Hong, (2019), Preparation and characterization of polylactic acid/polyaniline/nanocrystalline cellulose nanocomposite films, International Journal of Biological Macromolecules, DOI: https://doi.org/10.1016/j.ijbiomac.2019.09.233).

[81]   N.A. Sani, M.E.A. Manaf, J.A. Razak, M. I. Shueb and V.A. Doan, (2021), Thermal Characterization Of Indium Doped Zinc Oxide Coated Kenaf/Polyaniline/Polylactic Acid Hybrid Composite, Journal of Advanced Manufacturing Technology (JAMT), Vol. 15 (3), pp. 81-92.

[82]   J. P. Mofokeng, A. S. Luyt, T. Tabi, and J. Kovacs, (2011), Comparison of injection moulded, natural fibre-reinforced composites with PP and PLA as matrices, Journal of Thermoplastic Composite Materials, Vol. 25, pp. 927–948.

[83]   R. K Nagarale, G. S Gohil, V. K Shahi, G. S Trivedi, and R Rangarajan (2004). Preparation and electrochemical characterization of cation- and anion-exchange/polyaniline composite Membranes, Journal of Colloid and Interface Science, Vol. 277, pp. 162–171.

[84]   Y. Mo, W. Meng, Y. Xia, and X. Du, (2019), Redox-Active Gel Electrolyte Combined with Branched Polyaniline Nanofibers Doped with Ferrous Ions for Ultra-High-Performance Flexible Supercapacitors, Polymers (Basel). Vol. 11, pp. 1357-15.

[85]   N. Karaoğlan and Cuma Bindal  (2018), Synthesis and optical characterization of benzene sulfonic acid doped polyaniline, Engineering Science and Technology, An International Journal, Vol. 21, pp. 1152–1158.

[86]   S. Stafstrom and J. L. Bredas, (1987), Polaron lattice in highly conducting polyaniline: Theopriticxal and optical studies. Physical review Letter, Vol. 59, pp. 1464-1467.https://www.electronics-tutorials.ws/accircuits/parallel-resonance.html.

[87]   P. M. Grzeszczuk and P. Poks, (1995) , Analysis of charge transport impedance in the reduction of thin films of conducting polyaniline in aqueous trichloroacetic acid solutions, Journal of Electroanalytical Chemistry, Vol. 387, pp. 79-85.

[88]   A. Sikdar, S. K. Deb, A. Gogoi, A. Majumdar, P. Dutta, K. A. Reddy, and U. Narayan Maiti, (2020), Polyaniline–Graphene Hydrogel Hybrids via Diffusion Controlled Surface Polymerization for High Performance Supercapacitors, ACS Applied Nanomaterials, Vol. 3, pp. 12278–12287.

[89]   H. Wang, Z. Yu, MaherF. El-Kady, M. A. Matthew,  D. Kowal, M. Li, R.  B. Kaner,  (2019),  Graphene/oligoaniline based supercapacitors: Towards conducting polymer materials with high rate charge storage, Energy Storage Materials, Vol. 19, pp. 137-147.

[90]   N. M. Kocherginsky and Z. Wang, (2006), The role of ionic conductivity and interface in electrical resistance, ion transport and transmembrane redox reactions through polyaniline membranes, Synthetic Metals, Vol. 156, pp.1065–1072.

[91]   A. Wang, D. Jung,, D. Lee, and H. Wang, (2021), Impedance Characterization and Modeling of Subcellular to Micro-sized Electrodes with Varying Materials and PEDOT:PSS Coating for Bioelectrical Interfaces, ACS Applied Electronic Materials, Vol. 3, pp. 5226–5239.

[92]   R. Vinodh, R. S. Babu, S.  Sambasivam, C.  V. V. M. Gopi, S. Alzahmi, H. J. Kim, ALF de Barros, and I. M. Obaidat, (2022), Recent Advancements of Polyaniline/Metal Organic Framework (PANI/MOF) Composite Electrodes for Supercapacitor Applications: A Critical Review, Nanomaterials (Basel), Vol. 12, pp. 1511-20.

[93]   A. Varela-Álvarez, J. A. Sordo, and G. E. Scuseria, (2005), Doping of Polyaniline by Acid−Base Chemistry: Density Functional Calculations with Periodic Boundary Conditions, American Chemical Society, Vol. 127, pp. 11318–11327.

[94]   M. Tagowska, B. Pałys, and K. Jackowska, (2004), Polyaniline nanotubules - Anion effect on conformation and oxidation state of polyaniline studied by Raman spectroscopy, Synthetic Metals, Vol. 142, pp.:223-229.

[95]   H. Wang, J. Lin, and Z. X. Shen , (2016), Polyaniline (PANi) based electrode materials for energy storage and conversion,  Journal of Science: Advanced Materials and Devices, Vol. 1, pp. 225-255.

[96]   J. Ham, H.-U. Kim, and N. Jeon, (2023), Key Factors in Enhancing Pseudocapacitive Properties of PANI-InO$_x$ Hybrid Thin Films Prepared by Sequential Infiltration Synthesis, Polymers, Vol. 15, pp.1-9.

[97]   J. C. Martins, J. C. de M. Neto, R. R. Passos, L. A. Pocrifka  (2020),  Electrochemical behavior of polyaniline: A study by electrochemical impedance spectroscopy (EIS) in low-frequency,  Solid State Ionics, Vol. 346, pp. 115198-xxx.

[98]   I. Misnon, K. Manickavasakam, N. Nordin, and R. Jose, (2023), Fabrication and electrochemical evaluation of polyhedral PANI-coated $Co_3O_4$ electrode for supercapacitor application, International Journal of Applied Ceramic Technology, Vol.20, pp. 2030-2042.

[99]   P. C. Lekha, S. Subramanian, and P. Padiyan, (2009),  Investigation of pseudocapacitance effect and frequency dependence of ac impedance in Polyaniline-polyoxometalate hybrids, Journal of Materials Science,  Vol. 44, :pp. 6040-6053.

[100]  M. Panigrahi, and B. Adhikari,  Fundamentals On Polyaniline Based Composites, ISBN No. 9789390853403, 2021, DOI: 10.34256/ioriip2121, IOR INTERNATIONAL PRESS, pp. 1-43.

[101]  J. C.  Pandey and M. Singh, (2021), Dielectric polymer nanocomposites: Past advances and future prospects in electrical insulation perspective, SPE Polymers, Vol 2, pp. 236-256.

[102]  Z. Ahmad, 'Polymer Dielectric Materials', Dielectric Material. InTech, Oct. 03, 2012. DOI: 10.5772/50638.

[103]  H. G. Lee and H. G. Kim, (1990), Ceramic Particle Size Dependence of Dielectric and Piezoelectric Properties of Piezoelectric Ceramic-Polymer Composites, Journal of Applied Physics, Vol. 67, pp. 2024–2028.

[104]  M. Roy, J. K. Nelson, R. K. MacCrone, L. S. Schadler, C. W. Reed, R. Keefe, R, (2005), Polymer nanocomposite dielectrics-the role of the interface, IEEE Transection of Dielectric Electrical Insulator, Vol. 12, pp. 629–643.

[105]  Y. Rao, C. P. Wong, J. Qu, and Marinis, T., (2000), Self-consistent model for dielectric constant prediction of polymer–ceramic composite, In Proceedings of International Symposium on Advanced Packaging Materials, Vol. xxx, pp. 44–9.

[106]  A. B. Afzal, M. J. Akhtar, M. Nadeem, and M. M. Hassan, (2009), Investigation of Structural and Electrical Properties of Polyaniline/Gold Nanocomposites, The Journal of Physical Chemistry A, Vol. 113, pp. 17560–17565.

## Author's Short biography

| | |
|---|---|
|  | **Dr. Muktikanta Panigrahi** has completed MSc (Ravenshaw University), MTech (School of Materials Science & Engineering, IIT BHU, Varanasi), and PhD degree (Materials Science Centre, IIT Kharagpur). He has 10-years' experience in teaching and research. He is working as an Assistant Professor in the Department of Materials Science, Maharaja Sriram Chandra Bhanja Deo University (MSCBDU), Keonjhar campus, Keonjhar, Odisha, India. He has published Book Chapters/SCI Journals/Proceedings/etc. He has organised five International/National conferences. He has innovations/discoveries in the area of Geopolymer/MMCs/Ceramics/Polymers which is credit to the research. He has skilled in the field of Basification of Industrial Wastes, MMCs, Organic Semiconductor, Biodegradable polymer, Gas sensor. He has the member of International/National bodies (APA/MRS). |
|  | **Prof. Ratan Indu Ganguly** has completed BE and ME degree in Metallurgy from Calcutta University. He was awarded PhD from IIT Kharagpur. He has 50 years of experience in teaching (UG and PG level). He guided several PhD scholars. He received Kamini Gold medal in the year 1968 for his paper which was adjudged as the best paper published in IIM. He visited several countries on sponsored project programmes which include USA (Naval research), UK, Japan etc. He has done several consultancy works e.g., TISCO, L&T, Odisha cement, etc. He has completed several projects sponsored by government of India. He has completed an industry sponsored project i.e. development of floor and wall tiles from industrial waste such as fly ash. This was a NALCO sponsored programme. Prof Ganguly is now supporting a research project which relates to development of geopolymer from pond ash. |
| | **Dr. Radha Raman Dash** has completed PhD from Department of Materials & Metallurgical Engineering from IIT Kharagpur. He served CSIR-National Metallurgical Laboratory (NML), Jamshedpur as Senior Scientist. He was worked as Principal in, DRIEMS and BCET, Balasore, Orissa. Also, he served Dean (Research & Development), Gandhi Institute of Engg. & Technology, University, Gunupur, Orissa (continuing).  He has 55 years' experience. His research interests in many areas i.e., Foundry, Composite Materials, Corrosion, Ceramic Matrix Composites, Fractal Images and Advanced Materials. He has several publications in National/International Journals. He has 10 inventions/discoveries. He has special Recognition, Honours & Awards International and National level. He has many more innovations on his research works. |